Formulation of Common Spatial Patterns for Multi-task Hyperscanning BCI

Alicia Falcon-Caro, *Member, IEEE*, Sepehr Shirani, João Filipe Ferreira, *Member, IEEE*, Jordan J. Bird, and Saeid Sanei, *Senior Member, IEEE*

Abstract—**This work proposes a new formulation for common spatial patterns (CSP), often used as a powerful feature extraction technique in brain-computer interfacing (BCI) and other neurological studies. In this approach, applied to multiple subjects' data and named as hyperCSP, the individual covariance and mutual correlation matrices between multiple simultaneously recorded subjects' electroencephalograms are exploited in the CSP formulation. This method aims at effectively isolating the common motor task between multiple heads and alleviate the effects of other spurious or undesired tasks inherently or intentionally performed by the subjects. This technique can provide a satisfactory classification performance while using small data size and low computational complexity. By using the proposed hyperCSP followed by support vector machines classifier, we obtained a classification accuracy of 81.82% over 8 trials in the presence of strong undesired tasks. We hope that this method could reduce the training error in multi-task BCI scenarios. The recorded valuable motor-related hyperscanning dataset will be made available for public use to promote the research in this area.**

Index Terms—**Brain-computer interface, common spatial patterns, EEG, hyperscanning, multi-brain.**

I. INTRODUCTION

INTEREST in brain-computer interfaces (BCIs), which allow people to interact with the outside world through their brain signals, has grown in the last few decades [1], [2]. This can be associated with the development of cheaper high resolution non-invasive brain signal recording systems [3], [4], and the improvement of advanced signal processing [5], [6] and machine learning models [7], [8]. Most non-invasive BCIs are based on electroencephalography (EEG) due to its low cost, accessibility, high temporal resolution and portability

A. Falcon-Caro is with the Department of Computer Science, Nottingham Trent University, Nottingham, NG11 8NS, UK. (e-mail: alicia.falconcaro@ntu.ac.uk).

S. Shirani is with the Department of Computer Science, Nottingham Trent University, Nottingham, NG11 8NS, UK. (e-mail: sepehr.shirani2021@my.ntu.ac.uk).

J. F. Ferreira is with the Department of Computer Science, Nottingham Trent University, Nottingham, NG11 8NS, UK. (e-mail: joao.ferreira@ntu.ac.uk).

J. J. Bird is with the Department of Computer Science, Nottingham Trent University, Nottingham, NG11 8NS, UK. (e-mail: jordan.bird@ntu.ac.uk).

S. Sanei is with the Department of Computer Science, Nottingham Trent University, Nottingham, NG11 8NS, UK, and Department of Electrical and Electronic Engineering, Imperial College London, London SW7 2AZ, UK. (e-mail: s.sanei@imperial.ac.uk)

Fig. 1. A representation of an EEG hyperscanning recording with two subjects involved.

compared to other neuroimaging systems [9]. Although the use of these systems for other applications, such as in games [10], has become more prevalent, its main application remains in rehabilitation and as part of assistive technologies [11], [12].

Although recent studies on BCIs have shown promising results [13]–[18], these studies tend to rely on the use of large training datasets and ideal scenarios where the data is recorded in a controlled environment and the subjects are asked to constantly concentrate on a single motor-related task. This poses some challenges in the implementation of these systems in an uncontrolled environment and when working with non-ideal and smaller datasets where the brain is inherently engaged in multiple tasks.

EEG-based hyperscanning studies [19], also known as EEG-based multi-brain studies, have attracted researchers' attention in recent years. This technique, which involves simultaneous recording of EEGs from multiple brains, as shown in Fig. 1, allows researchers to study the inter-subject neural connections and how such connections are affected when multiple subjects interact with each other [20]. Currently, most hyperscanning studies have focused on the study of social interactions between humans, where the subjects' inter- and intra-brain connections change depending on the task they perform [21], [22]. Some multi-brain studies have also been implemented in game setups, as reviewed in [23]. However, in these implementations, although the brain waves from multiple subjects are recorded simultaneously, the signals from each subject are analyzed independently. Therefore, they should not be mistaken as pure EEG-based hyperscanning BCIs, where the signals from multiple subjects are recorded, preprocessed,

and jointly analysed.

To the best of our knowledge, the only attempt in EEG-based hyperscanning BCI is presented in [24], where the researchers developed a method that allowed the EEG signals from one subject to be modeled based on the EEG signals of another subject, assuming that the first subject follows the same task as the second subject. As discussed in the aforementioned paper and in [25], the development of an effective EEG-based hyperscanning BCI for a rehabilitation scenario could improve the accuracy and speed of the rehabilitation process while reducing the training error in the multi-task scenarios. As stated in [25], EEG-based hyperscanning BCIs for rehabilitation purposes have not been explored in depth yet due to the technical challenges that these systems present. Two main challenges are: 1) the difficulties of setting a motor rehabilitation scenario for hyperscanning, and 2) the complexity of analysing the EEG-based hyperscanning signals.

To help with the first challenge, we present and release a dataset containing data from several motor-related hyperscanning scenarios in this paper. To the best of our knowledge, only two hyperscanning datasets have been made publicly available at the time of writing [26], [27]. However, only [27] is EEG-based and none of them contains motor-related tasks that can be used to help develop new hyperscanning motor rehabilitation BCIs.

To overcome the second challenge, we developed a new filtering technique by reformulating the well-known common spatial patterns (CSP) method [28], which is tailor-made for hyperscanning data during collaborative activities, and obtains a satisfactory performance even with a smaller dataset than what is used in the related papers [29].

Given $X \in \mathbb{R}^{N \times L}$ as a segment of EEG signal, where N represents the number of channels and L the number of samples, the traditional CSP cost function can be formulated as:

$$J(\mathbf{W}) = \frac{\mathbf{W}^T \mathbf{X}_1^T \mathbf{X}_1 \mathbf{W}}{\mathbf{W}^T \mathbf{X}_2^T \mathbf{X}_2 \mathbf{W}} = \frac{\mathbf{W}^T \mathbf{C}_1 \mathbf{W}}{\mathbf{W}^T \mathbf{C}_2 \mathbf{W}} \qquad (1)$$

where $\mathbf{W}$ represents the filter coefficients that separate two classes of a brain activity, and $\mathbf{X}_1$ and $\mathbf{X}_2$ represent the signals from classes 1 and 2 respectively. In the classical CSP, $\mathbf{C}_1$ and $\mathbf{C}_2$ refer respectively to the covariance matrices for the subspaces of the signals from tasks 1 and 2 or those of the desired/undesired signals.

Since the hyperscanning data is not readily available and the recording of such data is difficult, it is essential to develop a system that can perform well for small datasets. To the best of our knowledge, this is the first time an EEG-based hyperscanning motor-related dataset is analyzed and classified. The proposed method, namely hyperCSP, enables the classification of EEG hyperscanning data dependent on whether the subjects are performing common tasks or not. This new method can also be used to classify motor-related multi-task scenarios where the tasks are all in common, even at the presence of strong undesired tasks, inherently or intentionally performed by the subjects. The technique is proposed for a scenario where the brain signals of two subjects are recorded simultaneously during the performance of common and uncommon tasks in

a multi-task scenario. This allows the system to be used with non-ideal data to establish a BCI that can perform favorably even in uncontrolled environments.

Section II and III explain the proposed CSP-based technique, Section IV-A describes the dataset used in this paper, and Section IV-B discuss the results obtained during the classification of common and undesired tasks. The code used in this paper as well as the dataset will be made available upon paper acceptance.

II. PROBLEM FORMULATION

In this section, we propose a novel approach for CSP-based spatial filtering as a feature extraction technique that can be used to classify the common task when the two subjects of an EEG hyperscanning study perform a common task, independently of what the common task is. The proposed hyperCSP technique is a reformulation of the well-known CSP method.

A. Hyperscanning Common Spatial Patterns

Our proposed hyperCSP aims at learning the spatial filters that maximize the variance of the EEG signals for when a common task is performed by multiple subjects while minimizing the variance for performing the uncommon tasks. In this way, the cost function for hyperCSP can be approximated as:

$$J(\mathbf{W}) = \frac{\mathbf{W}^T \big(\sum_{k=1}^{M} \mathbf{C}_k \big) \mathbf{W}}{\mathbf{W}^T \big(\sum_{j=1}^{M} \sum_{i=1, i \neq j}^{M} \mathbf{C}_{i,j}^g \big) \mathbf{W}} \qquad (2)$$

In this equation, the global correlation $\mathbf{C}_{1,2,...M}^g$ has been approximated by the sum of mutual correlations, i.e. $\mathbf{C}_{i,j}$.

Since $\mathbf{C}_{i,j} = \mathbf{C}_{j,i}$, eq. (2) can be simplified to:

$$J(\mathbf{W}) = \frac{\mathbf{W}^T \big(\sum_{k=1}^{M} \mathbf{C}_k \big) \mathbf{W}}{\mathbf{W}^T \big(\sum_{j=1}^{M-1} \sum_{i=j+1}^{M} \mathbf{C}_{i,j} \big) \mathbf{W}} \qquad (3)$$

where M is the number of subjects, $\mathbf{W}$ is the spatial filter, $\mathbf{C}_k$ is the spatial covariance matrix for subject k, and $\mathbf{C}_{i,j}$ is the mutual correlation matrix of subjects i and j.

The use of multiple heads in hyperscanning setting could enhance the classification accuracy, especially in uncontrolled environments where the subjects are free to perform undesired or non-relevant tasks. Here, due to resource limitations, we only work with two subjects. Therefore, the cost function for hyperCSP in (2) becomes:

$$J(\mathbf{W}) = \frac{\mathbf{W}^T (\mathbf{C}_1 + \mathbf{C}_2) \mathbf{W}}{\mathbf{W}^T \mathbf{C}_{1,2} \mathbf{W}} \qquad (4)$$

where $\mathbf{C}_1$ and $\mathbf{C}_2$ represent the spatial covariance matrices for Subjects 1 and 2 respectively, estimated as:

$$\mathbf{C}_k = \frac{\mathbf{X}_k \mathbf{X}_k^T}{\text{trace}(\mathbf{X}_k \mathbf{X}_k^T)} \qquad (5)$$

$\mathbf{X}_k = [\mathbf{x}_{k,1}, \mathbf{x}_{k,2}, ...\mathbf{x}_{k,L}]$ represents a trial of EEG signal for subject k, and L denotes the trial length. $\mathbf{X}_k^T$ represents the transpose of $\mathbf{X}_k$ and $\text{trace}(\mathbf{C})$ is sum of the diagonal elements

of matrix $\mathbf{C}$. On the other hand, in (4), $\mathbf{C}_{1,2}$ represents the linear mutual correlation matrix between the two subjects, defined as:

$$\mathbf{C}_{i,j} = \frac{\mathbf{X}_i \mathbf{X}_j^T}{\text{trace}(\mathbf{X}_i \mathbf{X}_j^T)} \tag{6}$$

where $\mathbf{X}_i$ and $\mathbf{X}_j$ refer respectively to the EEG signals of subjects i and j. Here, it is assumed that the signals have zero mean.

B. Solution to the HyperCSP Problem

To solve the maximization problem in (4), we use the Lagrange multiplier method, as shown in [30]. Following this method, the constrained problem in (4) is converted to an unconstrained problem:

$$\hat{J}_{\lambda,\mathbf{w}} = \mathbf{w}^T(\mathbf{C}_1 + \mathbf{C}_2)\mathbf{w} - \lambda(\mathbf{w}^T\mathbf{C}_{1,2}\mathbf{w} - 1) \tag{7}$$

where λ is the Lagrange multiplier. Then, to calculate the spatial filter $\mathbf{w}$, the derivative of $\hat{J}_{\lambda,\mathbf{w}}$ is taken and set equal to zero with respect to $\mathbf{w}$:

$$\frac{\partial \hat{J}_{\lambda,\mathbf{w}}}{\partial \mathbf{w}} = 2\mathbf{w}^T(\mathbf{C}_1 + \mathbf{C}_2) - 2\lambda\mathbf{w}^T\mathbf{C}_{1,2} = 0;$$
$$(\mathbf{C}_1 + \mathbf{C}_2)\mathbf{w} = \lambda\mathbf{C}_{1,2}\mathbf{w}; \tag{8}$$
$$\mathbf{C}_{1,2}^{-1}(\mathbf{C}_1 + \mathbf{C}_2)\mathbf{w} = \lambda\mathbf{w}$$

This leads to the eigenvalue problem. Therefore, we obtain the eigenvectors of $\mathbf{\Upsilon} = \mathbf{C}_{1,2}^{-1}(\mathbf{C}_1 + \mathbf{C}_2)$, and the spatial filter $\mathbf{w}$ is estimated as the row of $\mathbf{\Upsilon}$ eigenvector matrix corresponding to its largest eigenvalue. Such a filter also alleviates the effects of other undesired brain sources and artifacts.

III. METHODOLOGY

In this section, we introduce the steps performed in the experiments to process and analyze the raw EEG hyperscanning data. Before applying the method, the data are preprocessed to mitigate the effects of some EEG artifacts. The proposed hyperCSP is used to obtain the feature vectors that are given to the classifier. To classify the spatial feature matrix containing all the feature vectors, we apply a number of well-known classifiers to them.

The EEG hyperscanning data used in this experiment was recorded at 250Hz sampling frequency from two subjects simultaneously. It contains a total of 64 channels, 32 channels from each subject. The dataset is further explained in Section IV-A.

A. Data Preprocessing

The raw EEG hyperscanning data is preprocessed to remove any bad channels and some artifacts.

The data from both subjects are combined into a single data block $\mathbf{X}_{i+j}$ in the form of a $2N \times t$ matrix, where t represents the signal length. The first N channels are the EEG signals from subject one (i) while the other N channels are the EEG signals from subject two (j). Then, $\mathbf{X}_{i+j}$ is segmented into equal-length blocks based on the labels associated to

the EEG hyperscanning signals. In this way, we obtain EEG hyperscanning blocks in the form of a $2N \times L$ matrix, where L represents the segment length with a single label, either Task 1 or Task 2 activity, both potentially including uncommon (undesired) tasks.

Channel 27 from the first subject and channel 32 from the second subject (both distant from the motor area) present a low electrode-skin impedance value across most of the recording sessions, so they are considered bad channels. Therefore, these two channels from both subjects are removed, to maintain the symmetry between the two subjects' data. The locations of these channels are grey colored in Fig. 3. A Finite Impulse Response (FIR) bandpass filter of 1-50 Hz is applied to the data from both subjects to remove the baseline and reduce any possible power line noise. Then, an average re-referencing is applied to each subject's data separately. These preprocessing methods are applied with the help of the EEGLAB toolbox [31]. No other artifact removal procedure is applied to the data since the proposed hyperCSP method is also able to filter these undesired artifacts.

B. Feature Extraction

Once the signals from both subjects are preprocessed, we select an appropriate window size over which the signal is considered stationary and slide the window over all the signal segments. In this case, we selected a window size between 2.7s and 3.3s, depending on the length of each segment, with no overlap. For each sliding window, we apply (4)-(6) using the first N channels from subject i as $\mathbf{X}_i$ and the second N channels from subject j as $\mathbf{X}_j$. We obtain the right eigenvectors that leads to the best $\mathbf{W}$, as the desired spatial filters. Then, we sort $\mathbf{W}$ in descending order of the eigenvalues and apply the filters $\mathbf{W}$ corresponding to the largest eigenvalues to the signal window segment following the equations:

$$\mathbf{X}_i^f = \mathbf{W}^T\mathbf{X}_i \tag{9}$$

$$\mathbf{X}_j^f = \mathbf{W}^T\mathbf{X}_j \tag{10}$$

Given the projected signals, we apply a log-variance method similar to those in [17], [30] and [32] to extract the feature vector from the projected signals. Hence, we calculate the logarithm of the variances for the projected EEG window segment of each subject and normalize them to have zero mean and unit variance:

$$\mathbf{f}_i = \log\left(\frac{\text{var}(\mathbf{X}_i^f)}{\sum \text{var}(\mathbf{X}_i^f)}\right) \tag{11}$$

$$\mathbf{f}_j = \log\left(\frac{\text{var}(\mathbf{X}_j^f)}{\sum \text{var}(\mathbf{X}_j^f)}\right) \tag{12}$$

Once the feature vectors for all the signal segments are obtained, they are combined into a feature matrix, obtaining a $2N \times S$ matrix, where S represents the number of segments. This feature matrix is the input to our chosen classifiers. Fig. 2 summarizes the steps defined in this section, while Algorithm 1 represents the calculation of the feature matrix for each segment in pseudo code.
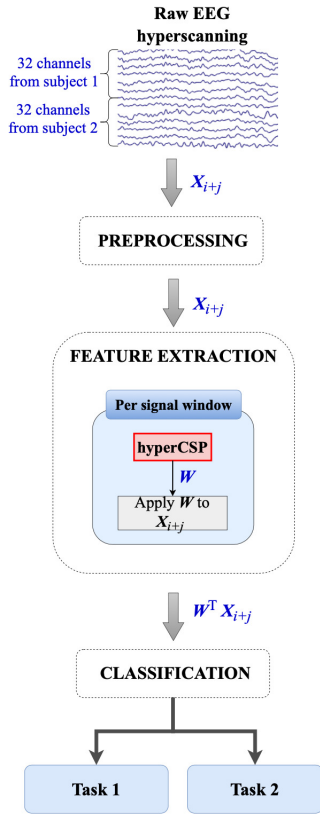
Fig. 2. A step-by-step illustration of the proposed method. The classification of the tasks is done in the presence of strong uncommon tasks.

Algorithm 1 Algorithm for HyperCSP

Input: EEG Segment (**EEG**: $2N \times L$)
   Prerequisites: Window Length D, Initial signal point P

1: **while** $D + P - 1 \leq$ Segment Length (L) **do**
2:     $\mathbf{X}_i = \mathbf{EEG}[1:N, P:P+D-1]$
3:     $\mathbf{X}_j = \mathbf{EEG}[N+1:2N, P:P+D-1]$
4:     $\mathbf{C1} = \dfrac{\mathbf{X}_i \cdot \mathbf{X}_i^T}{\text{trace}(\mathbf{X}_i \cdot \mathbf{X}_i^T)} + \dfrac{\mathbf{X}_j \cdot \mathbf{X}_j^T}{\text{trace}(\mathbf{X}_j \cdot \mathbf{X}_j^T)}$
5:     $\mathbf{C2} = \dfrac{\mathbf{X}_i \cdot \mathbf{X}_j^T}{\text{trace}(\mathbf{X}_i \cdot \mathbf{X}_j^T)}$
6:     $\mathbf{W} = \text{eigenvalues}(\mathbf{C1}, \mathbf{C2})$
7:     Sort $\mathbf{W}$ in descending order
8:     $\mathbf{X}_i^f = \mathbf{W}^T \cdot \mathbf{X}_i$
9:     $\mathbf{X}_j^f = \mathbf{W}^T \cdot \mathbf{X}_j$
10:    $\mathbf{f}_i =$ zero mean $\log(\text{var}(\mathbf{X}_i^f)/\sum \text{var}(\mathbf{X}_i^f))$
11:    $\mathbf{f}_j =$ zero mean $\log(\text{var}(\mathbf{X}_j^f)/\sum \text{var}(\mathbf{X}_j^f))$
12:    $P = P + D$
13: **end while**

Output: Normalized Feature Matrix $\{2N \times S\}$

C. Classification

Once the feature matrix is obtained, a classifier is selected and trained to classify the tasks performed by individuals.

To better validate the performance of the proposed hyper-CSP method, we applied three well-known classifiers that have shown promising results in previous CSP applications [33]. The chosen classifiers are linear kernel support vector machines (SVM), linear discriminant analysis (LDA) and k-nearest neighbors (KNN) with 3 neighbors.

The obtained feature matrices are divided into two subsets, one containing 75% for training and 15% for validation of the features matrices, and one for testing, containing the remaining 10% of the feature matrices. We used a 10-fold cross-validation.

IV. EXPERIMENTS

A. Dataset Description

This dataset will be made publicly available upon paper acceptance.

The data were recorded under the ethical approval from the Nottingham Trent University School of Science and Technology non-invasive Ethical Committee, under the application number $20/21/103$. All the volunteers gave their written consents.

The dataset contains the EEG hyperscanning data recorded from a total of four subjects, distributed in two pairs (Subjects 1 and 2, and Subjects 3 and 4). For each pair, all the experiments were recorded on the same day. All the subjects were healthy and between 20-30 years old. Out of the four subjects, there were three males and one female. The data were recorded using two g.tec Nautilus systems with 32 wet electrodes each, at 250Hz sampling frequency. Therefore, in total, 64 channels were recorded, 32 channels for each subject. The electrode locations for each system followed the standard 10-20 international EEG electrode placement, as shown in Fig. 3. Each system has a GND electrode located on the forehead of the subject and a reference on the right earlobe.

During each one of the five multi-task experiments, both subjects performed a common (similar to each other) task and an uncommon (different from each other) task simultaneously. The subjects performed all the experiments with their eyes open. Here, we describe each of the experiments.

During experiments 1 and 2, we recorded two trials for each and the subjects were asked to sit comfortably on their chairs one next to each other. However, for experiment 3, 4 and 5, only one trial per experiment was recorded and the subjects were standing one in front of each other.

Experiment 1: During this experiment, the two subjects were asked to open and close their right or left hands in a random order determined by a sequence of orders given to Subject 1. The left or right movement was also alternated with some randomly determined short free movement time. During the free movement time, the subjects were relaxing and free to move. During the movement, the whole arm was moved up and down following the opening and closing hands. The arm was moving down when opening the hand and up when closing it. Both subjects were asked to perform the movements at a slow pace and try to synchronize their movements. Subject 1 was leading the movement following the instructions received through a visual stimulus in a monitor, while Subject 2 was following Subject 1. Fig. 4a shows how the whole arm is moved when the hand is opened or closed.

Experiment 2: Like in the previous experiment, the two subjects were asked to open and close their right and left hands while moving the whole corresponding arm in a random
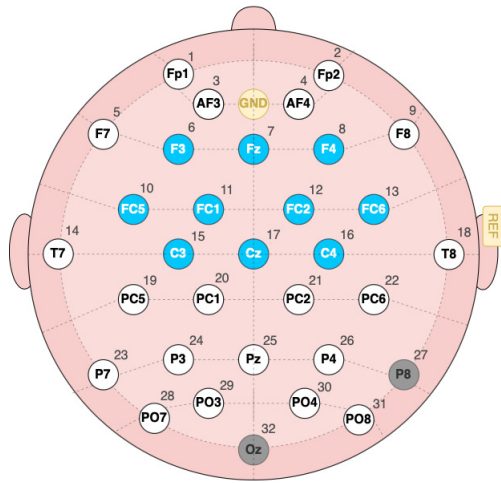
Fig. 3. An illustration of the electrode setup used for the experiment. The location of the electrodes follows the standard 10-20 international EEG electrode placement system for 32 electrodes. The highlighted electrodes in blue form a subsystem representing the motor area. The highlighted electrodes in grey represent channels 27 and 32 that have been removed during the preprocessing stage.
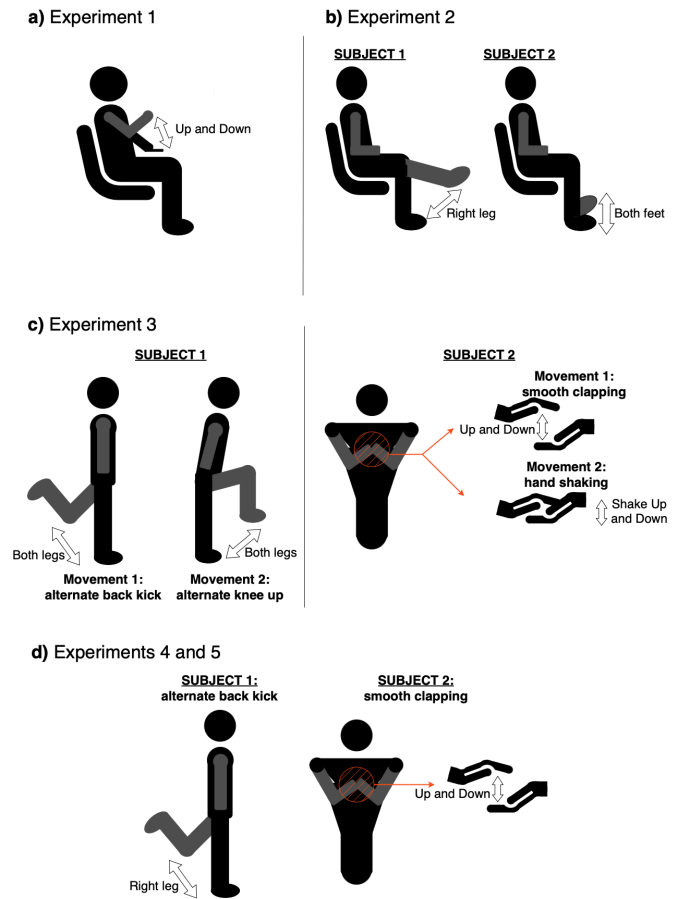

Fig. 4. The schematic of movement performed by the subjects during all the experiments. a) shows the open and close hand movement performed for experiment 1 and 2. b) shows the secondary movements performed by subjects 1 and 2 during experiment 2. c) illustrates the two secondary movements performed by each subject during experiment 3. d) illustrates the secondary movement performed by each subject during experiments 4 and 5.

order determined by a sequence of orders given to Subject 1. During this experiment, both subjects were also asked to simultaneously move another part of their body in a random order decided by themselves. Here, for the secondary movement, Subject 1 moves his right leg back and forth, while Subject 2 taps his feet. Fig. 4b shows the secondary movements performed by both subjects.

Experiment 3: During this experiment, both subjects were asked to open and close their both hands simultaneously following a slow motion. During this experiment, as opposed to experiments 1 and 2, only the hands were moving. Both subjects were asked to try to synchronize their opening and closing hand movements, and observation showed that the subjects were able to synchronize their movements most of the time. In a random order, Subject 1 was given three sets of instructions: to move freely his hands, to open and close his hands and to perform a secondary movement, while Subject 2 follows Subject 1. During the freely-moving time, both subjects were allowed to relax their hands and move them freely, as in previous experiments. During the secondary movement time, both subjects performed two movements each in a randomly self-decided order. Here, Subject 1 alternatively performed back kicks with each of his legs or alternatively moved one of his knees up. Subject 2 either performed a smooth hand shake between his both hands or smoothly clapped both his hands. Subject 2 performed continuous smooth movement of his arms and hands. Fig. 4c shows the secondary movements performed by both subjects. In these experiments, our main concern in on when both movements happen together.

Experiment 4: This experiment was a repetition of experiment 3, with a single change. Here, when the subjects were asked to perform the secondary movement, both subjects only performed a single movement instead of choosing between two movements. Subject 1 performed back kicks with his

right leg, while Subject 2 simulated a smooth continuous hand clapping. Fig. 4d shows the movement performed by both subjects during the secondary movement time.

Experiment 5: This experiment was a repetition of experiment 4, with a single change. During this experiment, both subjects, instead of only Subject 1, were given the instructions as to when to move freely, perform the secondary movement or open and close their hands. They were still asked to try to synchronize their movements.

B. Results

1) Classification of Common Multi-tasks: For the classification of common multi-tasks performed by two subjects in the presence of undesired tasks, a subset of the dataset described in Section IV-A is used. Only experiments 1 and 2 were used where the two subjects performed two separately labelled different common tasks and each performed a different (uncommon) task. Therefore, this subset of the dataset contains 8 trials. In here, we show the results obtained when applying hyperCSP and classifying the two common tasks: move right hand and move left hand, all at the presence of strong undesired tasks.
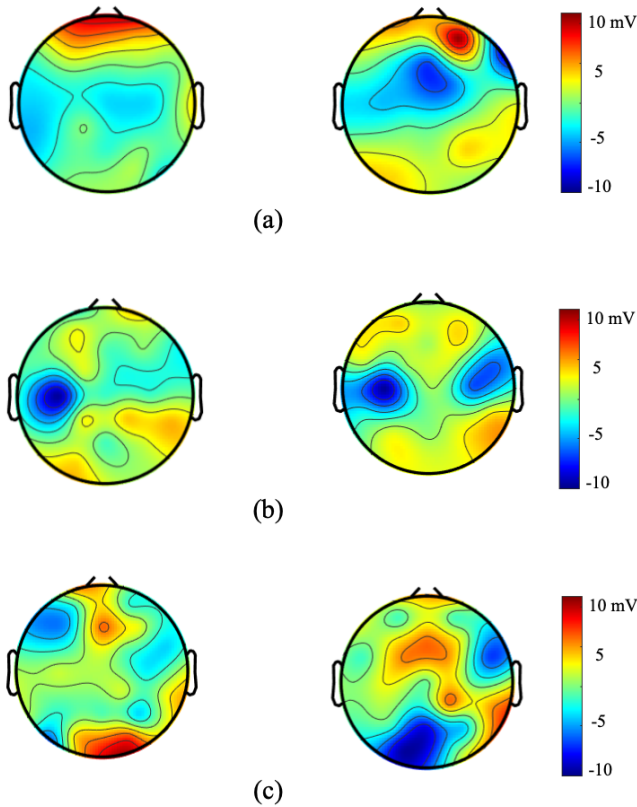
Fig. 5. The topoplots after applying CSP and hyperCSP to isolate the desired common task; (a) before any CSP filtering, (b) after applying CSP, and (c) after applying hyperCSP. In the left the activity in alpha band, and in the right the activity in beta band, have been demonstrated. The main conclusion is that the hyperCSP better isolates the brain common and desired prolonged activity.

To better validate the results, using the same dataset, we compare our results against results obtained using the traditional CSP, as defined in (1), using the data from one subject from each pair of subjects. This can show how a movement classification using EEG can be affected by undesired brain activities.

Fig. 5 shows the topoplots from Subject 1 of the first two trials of left-hand movement before and after applying hyperCSP and the comparison system. Since we are focusing on motor movements, the topoplots are represented for alpha and beta band frequencies (also known as alpha-mu and beta-mu). In Fig. 5 a), the topoplots before applying any CSP filtering are presented, and it can be appreciated that there is a mix of sources due to the undesired tasks performed by the subject while moving the left hand. In Fig. 5 b) and c), the topoplots after applying the filtering are presented, and it can be appreciated that hyperCSP is able to isolate the common task and obtain a clearer and more isolated alpha-mu and beta-mu. On the other hand, due to the presence of different sources, CSP is not able to clearly isolate the common task.

Table I shows the accuracy obtained for each of the mentioned methods used to validate our proposed system during the testing and training phases for each classifier. The results are the average validation accuracy and the standard deviation

of each system obtained after a 10-fold cross-validation. A maximum validation accuracy for each system, as well as the testing accuracy and the average F-score for the two classes, are obtained using the classifiers with the lowest validation error. The accuracy and F-score for the system are respectively defined as:

$$\text{Acc} = \frac{TP + TN}{TP + TN + FP + FN} \tag{13}$$

$$\text{F-score} = \frac{TP}{TP + \frac{1}{2}(FP + FN)} \tag{14}$$

where TP represents the true positives, TN represents the true negatives, FP represents the false positives, and FN represents the false negatives.

As explained in Section III-C, three classifiers are used. For consistency in the results, the parameters for the classifiers remained the same for the proposed and traditional methods.

As shown in Table I, for the classification of right and left hand movements, SVM results in the best performance for hyperCSP. We obtained an average validation accuracy of 62.77%, with a maximum validation accuracy of 76.47% and a testing accuracy of 81.82% for this model, which clearly shows the merit of hyperCSP for robust BCI.

2) Classification of Desired and Undesired Tasks: Now, we show that hyperCSP, similar to the traditional CSP, can also separate a relevant (desired task), which is in common between the participants, from irrelevant (undesired) tasks.

For the classification of desired (common) and undesired (uncommon) tasks for the two subjects, the full dataset involving 14 trials in total, described in Section IV-A, is used. For this experiment, we followed the same preprocessing steps and applied the same parameters as in the previous experiment.

In Table II, for most systems, the KNN classifier results in the best performance. Our method with the KNN classifier obtained an average validation accuracy of 64%, with a maximum validation accuracy of 70.97%, and a testing accuracy of 68.29%. This shows that our system is able to distinguish between tasks performed simultaneously at the presence of undesired (or random) individual tasks without any prior information about the tasks performed individually, even for a small dataset. In comparison, the classical CSP is not able to deal with separating the tasks at the presence of strong random or undesired tasks, while the hyperCSP can achieve a reasonable accuracy for such scenarios.

The results obtained in both experiments show that, given the same dataset, CSP is not able to distinguish between two tasks performed simultaneously at the presence of an undesired (or random) individual task without any prior information about the uncommon tasks performed individually. On the other hand, hyperCSP outperforms other popular feature detection methods, such as the traditional CSP, mainly because it benefits from more than one subject's EEG to marginalize the uncommon, unrelated, or spurious tasks.

Overall, we can conclude that the traditional CSP cannot work adequately when the brain is engaged in multi-task during BCI, while the hyperCSP system does with high accuracy. Due to limitations, in this paper we only work with

This article has been accepted for publication in IEEE Transactions on Biomedical Engineering. This is the author's version which has not been fully edited and content may change prior to final publication. Citation information: DOI 10.1109/TBME.2024.3356665

FALCON-CARO *et al.*: FORMULATION OF COMMON SPATIAL PATTERNS FOR MULTI-TASK HYPERSCANNING BCI 7

TABLE I

CLASSIFICATION ACCURACY DURING VALIDATION AND TESTING OF THE HYPERCSP AND THE COMPARISON SYSTEMS DURING THE CLASSIFICATION OF COMMON MULTI-TASKS.

	HyperCSP			CSP		
	SVM	LDA	KNN	SVM	LDA	KNN
Aveg. Validation Acc	**0.63±0.08**	0.60 ± 0.08	0.50 ± 0.08	0.44 ± 0.07	0.44 ± 0.07	**0.45 ± 0.07**
Max. Validation Acc	**0.76**	0.74	0.71	**0.59**	**0.59**	**0.59**
Testing Acc	**0.82**	0.73	0.45	**0.64**	**0.64**	0.36
F-score	**0.82**	0.73	0.45	**0.61**	**0.61**	0.34

TABLE II

CLASSIFICATION ACCURACY DURING VALIDATION AND TESTING OF THE HYPERCSP AND THE COMPARISON SYSTEMS DURING THE CLASSIFICATION OF DESIRED AND UNDESIRED TASKS.

	HyperCSP			CSP		
	SVM	LDA	KNN	SVM	LDA	KNN
Aveg. Validation Acc	0.53 ± 0.03	0.52 ± 0.03	**0.64 ± 0.03**	0.45 ± 0.05	0.45 ± 0.05	**0.47 ± 0.05**
Max. Validation Acc	0.58	0.59	**0.71**	**0.57**	0.53	**0.57**
Testing Acc	**0.71**	0.68	0.68	0.48	**0.57**	0.43
F-score	0.65	0.63	**0.67**	0.45	0.56	0.43

two subjects simultaneously. We expect that, by increasing the number of subjects in the hyperscanning setting, the training error will decrease. The hyperCSP may also be regularized to better incorporate the task properties.

V. CONCLUSIONS

In this paper, we propose a novel feature extraction technique based on CSP, namely hyperCSP, that can be used to analyze EEG hyperscanning data and classify different brain motor tasks when, during a synchronized multi-brain study, the subjects perform a common task at the presence of strong undesired tasks, similar to what we obtain in an uncontrolled environment. The results in this paper show that hyperCSP can achieve a satisfactory classification accuracy of 81.82% using a SVM classifier mainly because it benefits from the synchronized data from two subjects during a common movement task performance. The hyperCSP filter, **W**, can be applied to an individual's EEG to highlight the desired task and suppress all other undesired tasks. The results show that hyperCSP could improve the performance of a BCI. Various regularization techniques proposed for the conventional CSP by different researchers, such as in [29] and [34], can also be applied to hyperCSP to further improve its performance. Finally, with a larger dataset, the application of deep learning classification models such as deep neural networks could be considered in our future works, which may enhance the performance of our system, as shown in other studies [35], [36].

With this paper, we also provide an EEG motor task hyperscanning dataset, with the hope that the release of such dataset and the development of hyperCSP as an analysis method can enhance EEG hyperscanning BCI research.

REFERENCES

[1] A. Kawala-Sterniuk *et al.*, "Summary of over fifty years with brain-computer interfaces—a review," *Brain Sciences*, vol. 11, no. 1, p. 43, 2021.

[2] M. F. Mridha *et al.*, "Brain-computer interface: Advancement and challenges," *Sensors*, vol. 21, no. 17, p. 5746, 2021.

[3] M. Sawan *et al.*, "Wireless recording systems: From noninvasive EEG-NIRS to invasive EEG devices," *IEEE Transactions on Biomedical Circuits and Systems*, vol. 7, no. 2, pp. 186–195, 2013.

[4] Y. Huang *et al.*, "A wearable group-synchronized EEG system for multi-subject brain–computer interfaces," *Frontiers in Neuroscience*, vol. 17, 2023.

[5] S. Sanei *et al.*, "Advances in electroencephalography signal processing [life sciences]," *IEEE Signal Processing Magazine*, vol. 30, no. 1, pp. 170–176, 2013.

[6] A. Prochazka, O. Vysata, and V. Marik, "Integrating the role of computational intelligence and digital signal processing in education: Emerging technologies and mathematical tools," *IEEE Signal Processing Magazine*, vol. 38, no. 3, pp. 154–162, 2021.

[7] M. Mahmud *et al.*, "Applications of deep learning and reinforcement learning to biological data," *IEEE Transactions on Neural Networks and Learning Systems*, vol. 29, no. 6, pp. 2063–2079, 2018.

[8] X. Zhang *et al.*, "A survey on deep learning-based non-invasive brain signals: recent advances and new frontiers," *Journal of neural engineering*, vol. 18, no. 3, p. 031002, 2021.

[9] S. Sanei and J. A. Chambers, *EEG Signal Processing and Machine Learning*. John Wiley & Sons, 2021.

[10] G. A. M. Vasiljevic and L. C. De Miranda, "Brain-computer interface games based on consumer-grade EEG devices: A systematic literature review," *International Journal of Human-Computer Interaction*, vol. 36, no. 2, pp. 105–142, 2020.

[11] M. Zhuang *et al.*, "State-of-the-art non-invasive brain–computer interface for neural rehabilitation: A review," *Journal of Neurorestoratology*, vol. 8, no. 1, pp. 12–25, 2020.

[12] N. Robinson *et al.*, "Emerging trends in BCI-robotics for motor control and rehabilitation," *Current Opinion in Biomedical Engineering*, vol. 20, p. 100354, 2021.

[13] S. Lemm *et al.*, "Spatio-spectral filters for improving the classification of single trial EEG," *IEEE Transactions on Biomedical Engineering*, vol. 52, no. 9, pp. 1541–1548, 2005.

[14] G. Dornhege *et al.*, "Combined optimization of spatial and temporal filters for improving brain-computer interfacing," *IEEE Transactions on Biomedical Engineering*, vol. 53, no. 11, pp. 2274–2281, 2006.

[15] B. Blankertz *et al.*, "Optimizing spatial filters for robust EEG single-trial analysis," *IEEE Signal Processing Magazine*, vol. 25, no. 1, pp. 41–56, 2007.

[16] H. Kang, Y. Nam, and S. Choi, "Composite common spatial pattern for subject-to-subject transfer," *IEEE Signal Processing Letters*, vol. 16, no. 8, pp. 683–686, 2009.

[17] Z.-c. Tang *et al.*, "Classification of EEG-based single-trial motor imagery tasks using a B-CSP method for BCI," *Frontiers of Information Technology & Electronic Engineering*, vol. 20, no. 8, pp. 1087–1098, 2019.

[18] P. Gaur *et al.*, "A sliding window common spatial pattern for enhancing motor imagery classification in EEG-BCI," *IEEE Transactions on Instrumentation and Measurement*, vol. 70, pp. 1–9, 2021.

[19] P. R. Montague *et al.*, "Hyperscanning: simultaneous fMRI during linked social interactions," *Neuroimage*, vol. 16, no. 4, pp. 1159–1164, 2002.

[20] D. Liu *et al.*, "Interactive brain activity: review and progress on EEG-based hyperscanning in social interactions," *Frontiers in Psychology*, vol. 9, p. 1862, 2018.

[21] A. Czeszumski *et al.*, "Hyperscanning: a valid method to study neural inter-brain underpinnings of social interaction," *Frontiers in Human Neuroscience*, vol. 14, p. 39, 2020.

[22] M. Balconi and M. E. Vanutelli, "Cooperation and competition with hyperscanning methods: Review and future application to emotion domain," *Frontiers in Computational Neuroscience*, vol. 11, p. 86, 2017.

[23] A. Nijholt and H. Gürkök, "Multi-brain games: cooperation and competition," in *Universal Access in Human-Computer Interaction. Design Methods, Tools, and Interaction Techniques for eInclusion: 7th International Conference, UAHCI 2013, Held as Part of HCI International 2013, Las Vegas, NV, USA, July 21-26, 2013, Proceedings, Part I 7*. Springer, 2013, pp. 652–661.

[24] A. Falcon-Caro, M. Frincu, and S. Sanei, "A diffusion adaptation approach to model brain responses in an EEG-based hyperscanning study," in *2023 IEEE Statistical Signal Processing Workshop (SSP)*. IEEE, 2023, pp. 393–397.

[25] M. R. Short *et al.*, "EEG hyperscanning in motor rehabilitation: a position paper," *Journal of Neuroengineering and Rehabilitation*, vol. 18, no. 1, pp. 1–15, 2021.

[26] A. Bizzego *et al.*, "Dataset of parent-child hyperscanning functional near-infrared spectroscopy recordings," *Scientific Data*, vol. 9, no. 1, p. 625, 2022.

[27] M. A. Ramírez-Moreno, J. G. Cruz-Garza, and J. L. Contreras-Vidal, "Mobile EEG recordings of musical (jazz) improvisation," 2022.

[28] Z. J. Koles, M. S. Lazar, and S. Z. Zhou, "Spatial patterns underlying population differences in the background EEG," *Brain Topography*, vol. 2, pp. 275–284, 1990.

[29] H. Lu *et al.*, "Regularized common spatial pattern with aggregation for EEG classification in small-sample setting," *IEEE Transactions on Biomedical Engineering*, vol. 57, no. 12, pp. 2936–2946, 2010.

[30] K. Darvish Ghanbar *et al.*, "Correlation-based common spatial pattern (CCSP): A novel extension of CSP for classification of motor imagery signal," *Plos One*, vol. 16, no. 3, p. e0248511, 2021.

[31] A. Delorme and S. Makeig, "EEGLAB: an open source toolbox for analysis of single-trial EEG dynamics including independent component analysis," *Journal of Neuroscience Methods*, vol. 134, no. 1, pp. 9–21, 2004.

[32] M. Aljalal *et al.*, "Feature extraction of EEG based motor imagery using CSP based on logarithmic band power, entropy and energy," in *2018 1st International Conference on Computer Applications & Information Security (ICCAIS)*. IEEE, 2018, pp. 1–6.

[33] T. Nguyen *et al.*, "Classification of multi-class BCI data by common spatial pattern and fuzzy system," *IEEE Access*, vol. 6, pp. 27873–27884, 2018.

[34] F. Lotte and C. Guan, "Regularizing common spatial patterns to improve BCI designs: Unified theory and new algorithms," *IEEE Transactions on Biomedical Engineering*, vol. 58, no. 2, pp. 355–362, 2011.

[35] I. Sturm *et al.*, "Interpretable deep neural networks for single-trial EEG classification," *Journal of Neuroscience Methods*, vol. 274, pp. 141–145, 2016.

[36] M. Dehghani, A. Mobaien, and R. Boostani, "A deep neural network-based transfer learning to enhance the performance and learning speed of BCI systems," *Brain-Computer Interfaces*, vol. 8, no. 1-2, pp. 14–25, 2021.